



## Electrochromism based on the charge transfer process in a ferrocene–BODIPY molecule

Xiaodong Yin<sup>a</sup>, Yongjun Li<sup>a</sup>, Yuliang Li<sup>a,\*</sup>, Yulan Zhu<sup>c</sup>, Xueling Tang<sup>c</sup>, Haiyan Zheng<sup>a,b</sup>, Daoben Zhu<sup>a,\*</sup>

<sup>a</sup> Beijing National Laboratory for Molecular Sciences (BNLMS), CAS Key Laboratory of Organic Solids, Center for Molecular Sciences, Institute of Chemistry, Chinese Academy of Sciences, Beijing 100190, PR China

<sup>b</sup> Graduate University of Chinese Academy of Sciences, Beijing 100190, PR China

<sup>c</sup> Jiangsu Key Laboratory for Chemistry of Low-dimensional Materials, Huaiyin Teachers College, Huai'an, Jiangsu 223300, PR China

### ARTICLE INFO

#### Article history:

Received 17 June 2009

Received in revised form 5 August 2009

Accepted 6 August 2009

Available online 9 August 2009

#### Keywords:

Electrochromism

Organic metallic compound

Density functional theoretical calculation

Charge transfer

### ABSTRACT

A new type of donor–acceptor molecule **DiFc-B** combined ferrocene and BODIPY unit has been synthesized, and the NMR spectra, photophysical property, and electrochemical property were studied. The in situ spectro–electrochemical experiment was carried out, a notable absorption change had been observed under oxidative potential, and a recovery could happen under reductive potential and this process could repeat for several times. Such a phenomenon also happened when oxidative metal ion was added into the solution of **DiFc-B**. In order to study the mechanism of the electrochromism, the theoretical calculation was performed, and the result shows a D (ferrocene)– $\pi$ –A (BODIPY) system. The energy gap between the HOMO and LUMO had a good consistence with the electrochemical experiment and UV–vis data. The calculation of the frontier orbital belonging to the cation state of **DiFc-B** shows the directional change of the D– $\pi$ –A system, which supplied a theoretical basis of the electrochromism.

Crown Copyright © 2009 Published by Elsevier Ltd. All rights reserved.

## 1. Introduction

Organic electrochromic materials are a class of interesting molecules not only from the structural point of view, but also from the perspective of their novel electronic, optical, biological and chemical properties. At this stage, significant progress has been made in the synthesis of the electrochromic molecule materials.<sup>1</sup> However, most of the molecule materials are based on the conjugated molecules with heterocycles such as polythiophene, polypyrrole, polyanilines, viologen, etc.<sup>2–5</sup> The conjugated materials have a common character that the input part (or modulator) and the chromophore usually are shared, which leads to negative effect on their durability. Therefore, how to rationally design modulator–chromophore molecules that can avoid the problem above is very interesting. We prefer to design a D–A molecule system in which the charge transfer process can be switched by the modulator. The principles to such designs are lying in whether these molecules can occur the intramolecular charge transfer (ICT), which results in the appearance of the absorption band in the visible-light range,<sup>6–8</sup> and whether the reversible redox reactions of the modulator can switch the charge transfer process.

As we know, BODIPY derivatives, which have been widely employed as useful fluorescence probes and laser dyes, have many attractive characteristics.<sup>9–11</sup> In the previous works, the ICT process in the conjugated linked BODIPY derivatives has been investigated and showed application potential on the ‘naked eye’ sensors and switches.<sup>12,13</sup> And some reports have also indicated the advantage of the electrochemical reversibility of ferrocene moiety in the molecular systems.<sup>14</sup> However, the studies on the direct modulation of the ferrocene unit for electrochromism in a molecular system are still rare.<sup>15–17</sup> Herein, we designed and synthesized a new type of D– $\pi$ –A molecule system, which combined physical and chemical properties of electron donor ferrocene unit and electron acceptor BODIPY. The electrochemical reversibility of ferrocene was exploited for modulating the oxidative state of ferrocene to change the electron density distribution on the BODIPY, which leads to a change of ICT absorption property resulting in the electrochromism.

## 2. Results and discussion

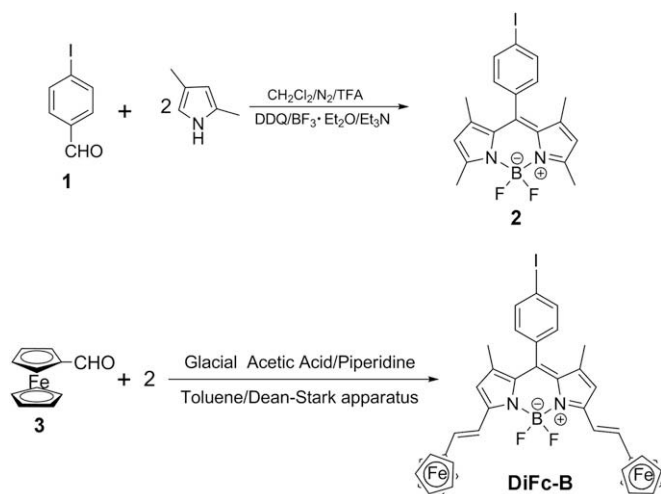
### 2.1. Synthesis of DiFc-B

Synthesis of **DiFc-B** is depicted in Scheme 1. Compound **2** was synthesized by condensation of compound **1** and dimethylpyrrole

\* Corresponding authors. Tel.: +86 10 62588934; fax: +86 10 82616576.

E-mail address: [ylli@iccas.ac.cn](mailto:ylli@iccas.ac.cn) (Y. Li).

catalyzed by acid. Direct condensation of **3** and **2** affords the novel compound of **DiFc-B** in the presence of piperidine and glacial acetic acid with a total yield of 15%.



Scheme 1. Synthesis of **DiFc-B**.

## 2.2. Photophysical properties

Figure 1 shows photophysical properties of **DiFc-B** and nude BODIPY in dichloromethane (DCM). **DiFc-B** has an absorption band in the range of 300–350 nm, which could be ascribed to the  $d_z^2 \rightarrow d_{xy}$  and  $d_{x^2-y^2} \rightarrow d_{xz}$  transition of the ferrocene moiety. The absorption band of BODIPY moiety in **DiFc-B** at about 500–550 nm has a slight red-shift compared with that of the individual BODIPY molecule, which is due to the extended conjugation. The absorption at 700 nm is assigned to the intramolecular charge transfer (ICT) band, and the strong charge transfer results in deep colour of the solution which plays a important role in our work. As we know, BODIPY dye is usually applied as fluorescent probes. But this compound is not emissive in its neutral state, which could be attributed to the strong charge transfer in the system. The strong charge transfer always induces the large red-shift of fluorescence, with an obvious quench simultaneously.

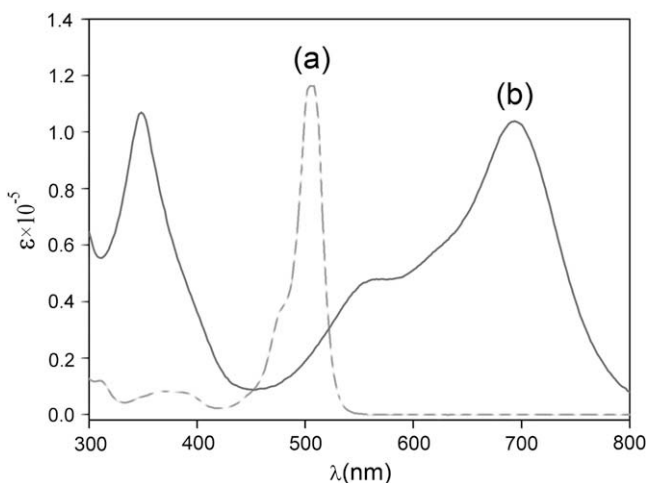


Figure 1. UV-vis absorption of compound **2** (a) and **DiFc-B** (b), concentration is  $5 \times 10^{-6}$  M.

## 2.3. Electrochemical properties

In order to investigate electrochemical properties of **DiFc-B**, the cyclic voltammogram (CV) measurements were carried out in deoxygenated DCM containing 0.1 M TBAPF<sub>6</sub>, and the results of electrochemical properties of **DiFc-B** are illustrated in Figure 2. The results indicate the redox peaks didn't move with the increasing of the scan rate, which shows the outstanding electrochemical reversibility of **DiFc-B**.<sup>18,19</sup> Two pairs of reversible one-electron redox peaks can be observed at about 1.0 V and –1.0 V, respectively, which could be ascribed to the BODIPY moiety.<sup>20</sup> The result indicates the BODIPY moiety has a push–pull system due to the electron transfer from N to B atom. The peak of the two-electron oxidation of ferrocene moieties locates at about 0.5 V, and splits into two peaks at lower scan rate. Differential pulse voltammogram (DPV) experiment gives a clear result, as shown in Figure 2a. When one of the ferrocene moieties was oxidized by an appropriate potential, the frontier orbital energy and the location of HOMO orbit were changed notably leading to influence the oxidative potential of the other ferrocene moiety. The oxidative potential of the ferrocene moieties in **DiFc-B** has an anodic shift compared with that of nude ferrocene in DCM (0.3 V) as shown in Figure 2b, indicating ferrocene moiety in **DiFc-B** bearing an electron-pulling effect from the BODIPY moiety.

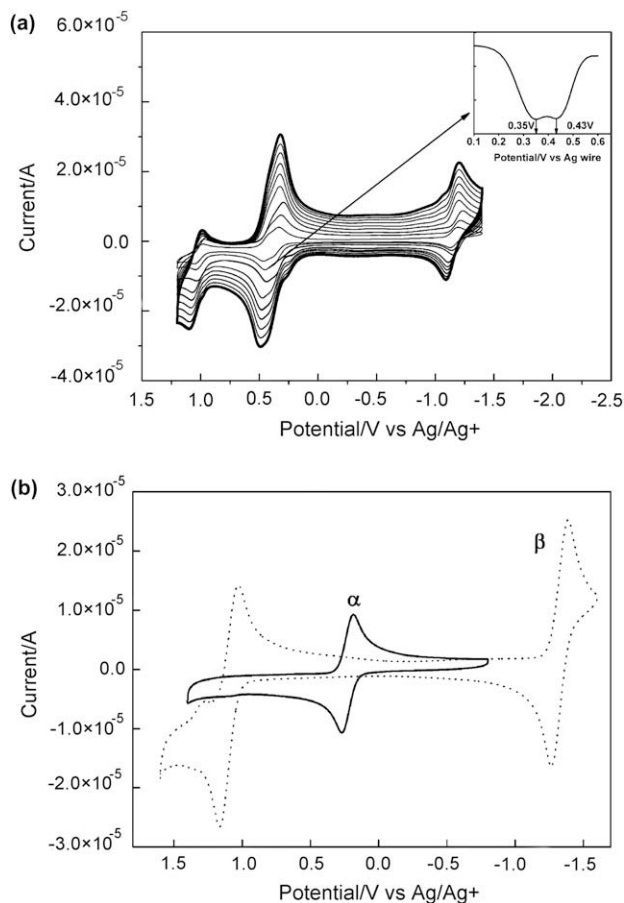


Figure 2. (a) The cyclic voltammogram of **DiFc-B**, scan rate from 50 mV/s (the inner line) to 800 mV/s (the outer line); differential pulse voltammogram (DPV) of **DiFc-B** (small image), scan from 0.1 V to 0.6 V. (b) the cyclic voltammogram of ferrocene (solid line) and BODIPY (dash line), scan rate: 200 mV/s. All measurements were carried out in deoxygenated DCM containing 0.1 M TBAPF<sub>6</sub>, glassy carbon electrode as working electrode, platinum wire as counter electrode and silver wire as reference electrode. The concentration of them was 0.002 M.

The cyclic voltammetry and spectral results are shown in Table 1. The spectral result has a slight blue shift compared with the CV result, which can be attributed to the hydrogen bond interaction between  $\text{CH}_2\text{Cl}_2$  and the solute.<sup>21</sup>

**Table 1**  
Electrochemical and photophysical data of **DiFc-B**

$E_p^a$ /V	$E_{pc}^b$ /V	HOMO <sup>c</sup> /eV	LUMO <sup>d</sup> /eV	Band gap(cv) <sup>e</sup> /eV	Band gap (UV-vis) <sup>f</sup> /eV
0.55	1.13	-5.13	-3.45	1.68	1.77

<sup>a</sup> Peak potential of first oxidation wave determined by cyclic voltammetry: 0.1 M TBAPF<sub>6</sub> as a supporting electrolyte in DCM, glassy carbon electrode as working electrode and Pt as counter electrode, scan rate in 50 mV/s.

<sup>b</sup> Peak potential of first reduction wave.

<sup>c</sup> Calculated according to  $E_{\text{HOMO}} = -e(E_{\text{ox}}) + 4.58$  as the potential of Ag electrode is 4.58 V below vacuum level.<sup>22,23</sup>

<sup>d</sup> Calculated according to  $E_{\text{LUMO}} = -e(-E_{\text{red}} + 4.58)$ .

<sup>e</sup> Calculated from  $E_{\text{gap}} = E_{\text{HOMO}} - E_{\text{LUMO}}$  (from CV).

<sup>f</sup> Band gap obtained from UV absorption onset value, calculated as  $E_{\text{gap}} = hc/\lambda_{\text{onset}} = 1240/\lambda_{\text{onset}}$ .

## 2.4. Electrochromic experiment

The in situ spectrochemical experiments were carried out in DCM with 0.1 M of TBAPF<sub>6</sub> as supporting electrolyte, and using light transparent platinum gauze (100 mesh, 0.07 mm diameter) as a working electrode. For the oxidative potential of the ferrocene is at about 0.5 V (vs Ag wire) and the BODIPY moiety is at about 1.0 V (vs Ag wire), an oxidative potential of 0.7 V (vs Ag wire) was applied. The time-depending UV spectra are shown in Figure 3a. Under the oxidative potential, the intensity of ICT absorption band at 700 nm reduces gradually. At the same time, a new absorption peak at about 600 nm were observed, resulting in a colour change from deep blue to red. The absorption band of BODIPY core at 550 nm was unchanged in the process. When a reductive potential (0 V vs Ag wire) was applied, an opposite transformation could be observed as shown in Figure 3b. In the first cycle, both of the ICT absorption band at 700 nm and the ferrocene moieties absorption band at 350 nm have a recovery of 80%, and the colour is also recovered. The 20% of loss might be due to the adherence of solute on the Pt-grid electrode. The oxidation and reduction process were carried out for several cycles without any fatigue as shown in Figure 3c, which indicates good reversibility.

## 2.5. Oxidative metal ion responding experiment

Except for the electrochromic experiment, we also found that the compound could respond to the oxidative metal ion like  $\text{Cu}^{2+}$ . Notable changes in the absorption spectra of **DiFc-B** were observed upon addition of an increasing amount of  $\text{Cu}^{2+}$  ion. The absorption maximum at 690 nm in the visible region decreased in intensity and was accompanied by the increasing of the absorption band at 550 nm as shown in Figure 4. The latter band is characteristic of absorption band of BODIPY core. The results are similar to that of the electro oxidation at potential of 0.7 V (vs Ag wire).

## 2.6. Quantum chemical calculations

To investigate the mechanism of electrochromism, quantum chemistry calculation was performed using density functional theory (DFT) methods employing the Amsterdam-density-functional (ADF 2006.01) program package. Geometric structures of the complex have been investigated by BP86/TZ2P methods without any constraint as shown in Figure 5a.<sup>24</sup> As expected, the **DiFc-B** with conjugated connection between two parts has planar

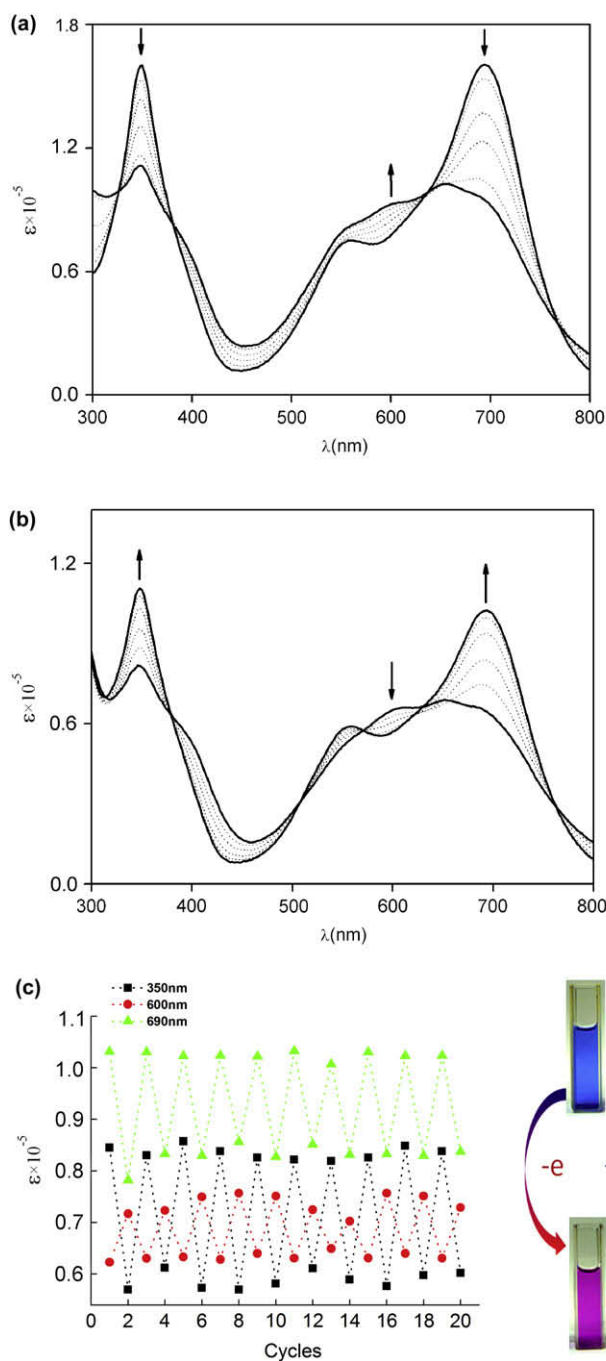


**Figure 3.** Spectro electrochemistry of **DiFc-B**. (a) Spectra change under 0.7 V versus Ag/Ag<sup>+</sup> (from neutral state to oxidative state), (b) spectro change under 0 V versus Ag/Ag<sup>+</sup> (from oxidative state to neutral state), (c) cycles of electrochemical modulation. The concentration of **DiFc-B** is  $5 \times 10^{-6}$  M.

configuration, and the benzene ring linked with the *meso* position of BODIPY has a dihedral angle of about 60°. The trans-conformation of the double bond between Fc moiety and BODIPY is consistent with the NMR result ( $J = 16$  Hz).

In order to study the ascription of UV-vis absorption of **DiFc-B**, simulated UV-vis absorption of **DiFc-B** was calculated by using TDDFT based on the optimized configuration,<sup>25</sup> and the result was shown in Figure 5b and Table 2. The result indicated that the longest wavelength of the absorption located on about 800 nm (1.47 eV), which match up well to the experiment result (1.77 eV,  $\Delta E = 0.3$  eV), and this absorption wave is mainly contributed by the transition from HOMO to LUMO (57%).

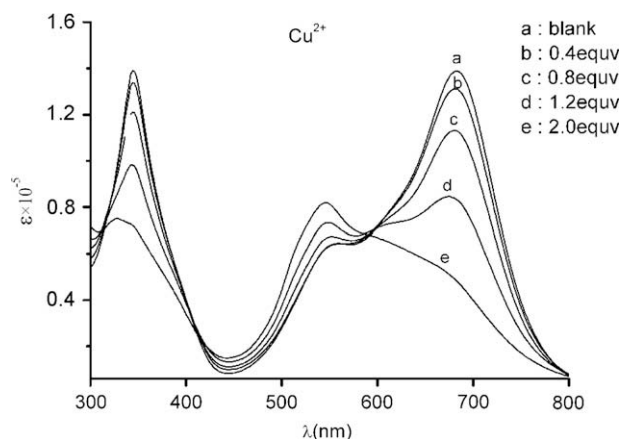


**Figure 4.** UV-vis absorption spectra of **DiFc-B** in the presence of different amounts of copper(II) perchlorate. Arrows indicate bands that change during the experiment. The concentration of **DiFc-B** is  $5 \times 10^{-6}$  M.

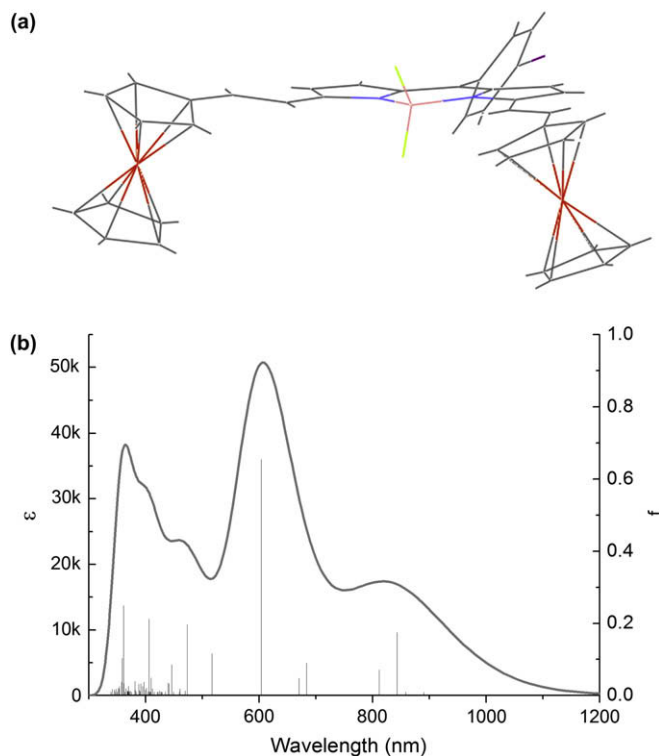


**Figure 5.** (a) Calculated configuration of **DiFc-B**; (b) Simulated UV-vis absorption of **DiFc-B**.

**Table 2**  
Data of simulate UV-vis absorption of **DiFc-B**

State	Energy (eV)	$f^a$	Major contribution
3A	1.47	0.16	H->L(57%) H-4->L(30%) H-1->L(11%)
7A	2.05	0.64	H-4->L(41%) H->L(28%) H-6->L(22%)
9A	2.62	0.19	H-8->L(47%) H->L+1(30%)
30A	3.05	0.20	H-4->L+1(20%) H->L+1(11%)
57A	3.43	0.24	H->L+8(19%) H-16->L(12%)

$f^a$  intensity factor.

HOMO and LUMO of **DiFc-B** are also calculated through the ADF calculation with TZP basis set as shown in Figure 6(left). HOMO and LUMO of **DiFc-B** orbitals are localized on the ferrocene and BODIPY moiety, respectively, which indicate that the ferrocene moiety is donor and the BODIPY part is acceptor in the **DiFc-B** molecule.

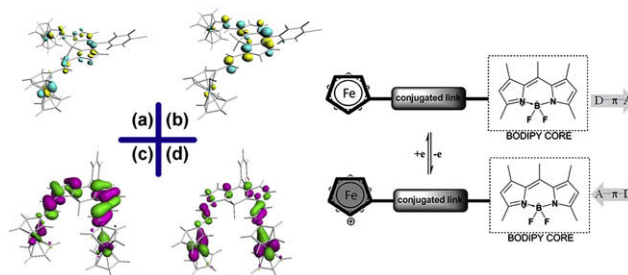


**Figure 6.** Left: Calculated frontier orbitals (a) HOMO of **DiFc-B**, (b) LUMO of **DiFc-B**, (c) HOMO of **DiFc<sup>2+</sup>-B**, (d) LUMO of **DiFc<sup>2+</sup>-B**. Right: sketch of redox process of D- $\pi$ -A system.

The calculation of the cation state of **DiFc-B** was also performed. The HOMO and LUMO orbitals are mainly localized on BODIPY part and ferrocene moiety, respectively, which means the direction of D- $\pi$ -A structure in the cation state is reversed to that of the neutral state. The results indicate the transformation is able to change the electron density distribution upon the molecular system leading to the electrochromism. The sketch of the redox process of **DiFc-B** is illustrated in Figure 6(right).

### 3. Conclusion

In conclusion, we demonstrated a new type of D- $\pi$ -A system combined with ferrocene and BODIPY. The electrochemical reversibility of ferrocene was exploited for modulating the oxidative state of ferrocene for changing successfully the electron density distribution on the BODIPY molecule, which result in an outstanding switch of ICT absorption to achieve the aim of electrochromism.

## 4. Experimental

### 4.1. Methods and materials

The ferrocenylaldehyde was purchased from the Tianjin Pharmcn Co. Ltd., 2,4-dimethylpyrrole and copper (II) perchlorate were purchased from Aldrich Co. Ltd. Tetra-*n*-butylammonium hexfluorophosphate (TBAPF<sub>6</sub>) used as the supporting electrolyte for the electrochemical measurement was obtained from Alfa-Aesar Co. Ltd., recrystallized and dried in vacuo prior to use. All the solvents used in electrochemical measurements and photophysical measurements were of HPLC grade quality, purchased and used without further purification unless otherwise noted. All the solvents and reagents used in the synthesis such as trifluoro acetic acid (TFA), triethyl ammonium (TEA), dichloromethane (DCM) and piperidine were purchased and purified by standard methods.

### 4.2. Synthesis and characterization

**4.2.1. 4,4'-Difluoro-8-(4-iodo) phenyl-1,3,5,7-tetramethyl-4-bora-3a,4a-diaza-s-indacene (2)**<sup>26</sup>. This compound was synthesized following literature method with some improvement. Under nitrogen atmosphere, to 1 L dichloromethane was added 1.8 g 4-iodobenzaldehyde and the mixture was stirred for 20 min. Then, 1.47 g 2,4-dimethylpyrrole was added to that mixture. After 10 min, a drop of trifluoro acetic acid was added, and the mixture was stirred for 5–6 h in the dark. Then, a solution of dichloro dicyane

benzoquinone (2 g) in dichloromethane was added dropwise to the deep red mixture during 2 h period. After stirring for another 30 min, TEA (6 mL) and  $\text{BF}_3 \cdot \text{OET}_2$  (6 mL) were added to the mixture, stirred overnight. The reaction was quenched by adding water, and the water layer was removed. The organic layer was concentrated on the rotary evaporator, and the residue was subjected to column chromatography (silica gel,  $\text{CH}_2\text{Cl}_2/\text{Hexane}=1:3$ ) to afford orange crystal (1.4 g, 40%).

**4.2.2. 3,5-[2'-(Ferrocenyl) ethenyl]-4,4'-difluoro-8-(4-iodo) phenyl-1,3,5,7-tetramethyl-4-bora-3a, 4a-diaza-s-indacene.** To a solution of 4,4-Difluoro-1,3,5,7-tetramethyl-8-(4-iodo-phenyl)-4-bora (450 mg, 1 mmol) and ferrocenealdehyde (2.14 g, 10 mmol) in 40 mL of toluene were added glacial acetic acid (375  $\mu\text{L}$ ), piperidine (450  $\mu\text{L}$ ) and small amount of  $\text{Mg}(\text{ClO}_4)_2$ . The resulting mixture was refluxed, and the water formed during the reaction was removed azeotropically by heating overnight in a Dean–Stark apparatus. The solvent was removed under vacuum, and the residue was purified by silica gel column chromatography ( $\text{CH}_2\text{Cl}_2$  to  $\text{CH}_2\text{Cl}_2/\text{MeOH}=100:2$ ). The blue fraction was collected to afford a dark blue solid (261 mg, 31%).  $^1\text{H}$  NMR (400 MHz,  $\text{CDCl}_3$ ):  $\delta$  1.46 (s, 6H), 4.20 (s, 10H), 4.46 (s, 4H), 4.66 (s, 4H), 6.52 (s, 2H), 7.07 (d, 2H,  $J=16.1$  Hz), 7.08 (d, 2H,  $J=8.2$  Hz), 7.26 (d, 2H,  $J=16.1$  Hz), 7.84 (d, 2H,  $J=8.2$  Hz).  $^{13}\text{C}$  NMR (100 MHz,  $\text{CDCl}_3$ ):  $\delta$  15.04, 68.31, 69.86, 70.67, 82.29, 94.68, 117.66, 130.71, 132.84, 135.37, 136.86, 138.30, 141.07, 152.73, 171.27. MALDI-TOF MS  $m/z$  842.1 ( $\text{C}_{41}\text{H}_{34}\text{BF}_2\text{Fe}_2\text{IN}_2$  requires 842.05). Elemental analysis calcd (%) for **DiFc-B**: C, 58.48; H, 4.07; N, 3.33. Found: C, 58.12; H, 3.98; N, 3.56.

### 4.3. Photo physical & electrochemical measurements

The UV–vis absorption spectrums were measured on a Hitachi U-3010 spectrometer. Electrochemical measurements such as cyclic voltammetry (CV) and differential pulse voltammetry (DPV) were carried out with a CHI660B electrochemical workstation using a three-electrode arrangement in a single cell with a Pt wire counter electrode, a glassy carbon working electrode, and an Ag wire reference electrode. The sample solutions contained the compound **DiFc-B** ( $1.0 \times 10^{-3}$  M) and 0.1 M TBAPF<sub>6</sub> as the supporting electrolyte in DCM. UV–vis spectro-electrochemical experiments were performed with a spectro-electrochemical quartz cell (path-length of 0.5 mm) using a three-electrode arrangement: light transparent platinum gauze (100 mesh, 0.07 mm diameter) as a working electrode, a platinum wire counter electrode, and an Ag wire reference electrode. Potentials were applied with a CHI660B electrochemical workstation. The electrochemical reaction was monitored with a Hitachi U-3010 spectrometer. All electrochemical measurements were carried out under an atmospheric pressure of nitrogen.

### 4.4. Method of quantum chemical calculations

In order to get information about the optimized geometry conformation and frontier orbital, quantum calculation with Amsterdam-density-functional (ADF 2006.01) program package have been carried out. The ground state geometry configuration of **DiFc-B** was optimized by the gradient corrected BP functional. For

describing the geometry and orbital energy of the compound precisely, TZP basis set was used for all atoms in the calculations.

### Acknowledgements

This work was supported by the National Nature Science Foundation of China (20831160507, 20721061, 20671038) and the National Basic Research 973 Program of China.

### Supplementary data

Characterization data such as  $^1\text{H}$ ,  $^{13}\text{C}$  NMR, and mass spectra for synthesized compounds, could be found in the online version. Supplementary data associated with this article can be found in the online version, at doi: 10.1016/j.tet.2009.08.008.

### References and notes

- (a) Schwendeman, I.; Hwang, J.; Welsh, D. M.; Tanner, D. B.; Reynolds, J. R. *Adv. Mater.* **2001**, *13*, 634–637; (b) Saap, S. A.; Sotzing, G. A.; Reddinger, J. L.; Reynolds, J. R. *Adv. Mater.* **1996**, *8*, 808–811; (c) Groenendaal, L. B.; Jonas, F.; Freitag, D.; Pielartzik, H.; Reynolds, J. R. *Adv. Mater.* **2000**, *12*, 481–494.
- Thompson, B. C.; Kim, Y. G.; McCarley, T. D.; Reynolds, J. R. *J. Am. Chem. Soc.* **2006**, *128*, 12714–12725.
- Sapp, S. A.; Sotzing, G. A.; Reynolds, J. R. *Chem. Mater.* **1998**, *10*, 2101–2108.
- Nielsen, C. B.; Angerhofer, A.; Abboud, K. A.; Reynolds, J. R. *J. Am. Chem. Soc.* **2008**, *130*, 9734–9746.
- Nishikitani, Y.; Uchida, S.; Asano, T.; Minami, M.; Oshima, S.; Ikai, K.; Kubo, T. *J. Phys. Chem. C* **2008**, *112*, 4372–4377.
- Das, D. K.; Mukherjee, A. K.; Gutman, I. *J. Chem. Sci.* **1990**, *102*, 759–767.
- Morales, R. G. E.; Vargas, V.; Hernández, C. *Spectroscopy* **1997**, *13*, 201–206.
- Kim, K. S.; Noh, S. B.; Katsuda, T.; Ito, S.; Osuka, A.; Kim, D. *Chem. Commun.* **2007**, 2479–2481.
- van Patten, P. G.; Shreve, A. P.; Lindsey, J. S.; Donohoe, R. J. *J. Phys. Chem. B* **1998**, *102*, 4209–4216.
- Wagner, R. W.; Lindsey, J. S.; Seth, J.; Palaniappan, V.; Bocian, D. F. *J. Am. Chem. Soc.* **1996**, *118*, 3996–3997.
- Lammi, R. K.; Wagber, R. W.; Ambrose, A.; Diers, J. R.; Bocian, D. F.; Holten, D.; Lindsey, J. S. *J. Phys. Chem. B* **2001**, *105*, 5341–5352.
- Rurack, K.; Kollmannsberger, M.; Daub, J. *Angew. Chem., Int. Ed.* **2001**, *40*, 385–387.
- Yuan, M.; Li, Y.; Li, J.; Li, C.; Liu, X.; Lv, J.; Xu, J.; Liu, H.; Wang, S.; Zhu, D. *Org. Lett.* **2007**, *9*, 2313–2316.
- (a) *Ferrocene*; Togni, A., Hayashi, T., Eds.; Wiley-VCH: Weinheim, Germany, 1995; (b) Anne, A.; Bouchardon, A.; Moiroux, J. *J. Am. Chem. Soc.* **2003**, *125*, 1112–1113; (c) Caballero, A.; Tárraga, A.; Velasco, M. D.; Espinosa, A.; Molina, P. *Org. Lett.* **2005**, *7*, 3171–3174.
- Santhosh, N. S.; Sundararajan, G. *Org. Lett.* **2006**, *8*, 605–608.
- Martínez, R.; Ratera, I.; Tárraga, A.; Molina, P.; Veciana, J. *Chem. Commun.* **2006**, 3809–3811.
- Rochford, J.; Rooney, A. D.; Pryce, M. T. *Inorg. Chem.* **2007**, *46*, 7247–7249.
- Electrochemical Methods: Fundamentals and Applications*, 2nd ed.; Bard, A. J., Faulkner, L. R., Eds.; John Wiley & Sons: New York, NY, 2000.
- Nicholson, R. S.; Shain, I. *Anal. Chem.* **1964**, *36*, 706–723.
- Hattori, S.; Ohkubo, K.; Urano, Y., et al. *J. Phys. Chem. B* **2005**, *109*, 15368–15375.
- Wang, S. L.; Gao, G. Y.; Ho, T. I.; Yang, L. Y. *Chem. Phys. Lett.* **2005**, *415*, 217–222.
- Kawaguchi, K.; Nakano, K.; Nozaki, K. *Org. Lett.* **2008**, *10*, 1199–1202.
- Kawaguchi, K.; Nakano, K.; Nozaki, K. *J. Org. Chem.* **2007**, *72*, 5119–5128.
- (a) Becke, A. D. *Phys. Rev. A: At., Mol., Opt. Phys.* **1988**, *38*, 3098–3100; (b) Perdew, J. P. *Phys. Rev. B: Condens. Matter* **1986**, *33*, 8822–8824.
- van Gisbergen, S. J. A.; Snijders, J. G.; Baerends, E. J. *Comput. Phys. Commun.* **1999**, *118*, 119–138.
- (a) Treibs, A.; Kreuzer, F.-H. *Liebigs Ann. Chem.* **1968**, *718*, 208–223; (b) Li, L.; Han, J.; Nguyen, B.; Burgess, K. *J. Org. Chem.* **2008**, *73*, 1963–1970.